^{209}Bi NQR and Magnetic Properties of Bismuth Oxide-Based Compounds

E. A. Kravchenko, V. G. Orlov[a], Suan Hai Fam, and Yu. F. Kargin

Institute of General and Inorganic Chemistry, Russian Academy of Sciences, Leninskii pr. 31, Moscow 117907, Russia
[a] Russian Scientific Center, Kurchatov Institute, Kurchatov sq. 1, Moscow 123182, Russia

Z. Naturforsch. **53a,** 504–513 (1998); received January 26, 1998

The NQR line shapes of ^{209}Bi in the α-Bi_2O_3-based mixed oxides $Bi_2O_3 \cdot 2M_2O_3$ (M = Al, Ga). $Bi_2O_3 \cdot 3GeO_2$, and $2Bi_2O_3 \cdot 3GeO_2$ are recorded in zero and weak magnetic fields ($H_{ext} < 500$ Oe) and compared with the results of computer simulation. Splittings and line shape asymmetry, exhibited by the resonances, suggest that internal magnetic fields, similar to those earlier reported for α-Bi_2O_3 and Bi_3O_4Br, may exist in these compounds.

In the spectra of single crystal $Bi_4Ge_3O_{12}$, the line multiplicity in external magnetic fields is higher than simulated, which might results from domains in the crystal.

In external magnetic fields a notable increase in the line intensity was observed, the effect depending on the mutual orientation of the EFG axes and the fields perturbing the nuclear spin system.

Key words: ^{209}Bi NQR; Internal Magnetic Field; Line Shape; Applied Magnetic Field; Computer Simulation.

Introduction

As was reported in [1], the ^{209}Bi NQR spectra of α-Bi_2O_3 and Bi_3O_4Br are split in zero external magnetic field. The splittings showed the typical Zeeman patterns, consistent with the existence of internal magnetic fields of the order of 200 G. In addition to the Zeeman splittings, a considerable increase in intensity of the ^{209}Bi resonances was observed in weak (below 500 Oe) static magnetic fields [1].

The results, obtained using the μSR-technique [2], were explained by internal magnetic fields existing in the intersticials of the α-Bi_2O_3 lattice. More recent SQUID measurements [3] on α-Bi_2O_3 over a wide range of external magnetic fields and temperatures revealed numerous anomalies in its magnetic properties, which were not observed in strong magnetic fields applied in traditional experiments, e.g. the Faraday method. Anomalies in the physical properties of α-Bi_2O_3 were also revealed by calorimetric, electric conductivity, and permeability measurements [4] at 450–570 K.

Thus the results of many experiments show that the magnetic properties of α-Bi_2O_3 and Bi_3O_4Br are unexpectedly complicated. In this work, a systematic search for new Bi_2O_3-based compounds, exhibiting unconventional ^{209}Bi NQR spectra, was undertaken.

Experiment

This paper deals with mixed oxides comprising, apart from α-Bi_2O_3 other Main Group metal oxides, namely, $Bi_2O_3 \cdot 2M_2O_3$ (M = Al, Ga), $Bi_2O_3 \cdot 3GeO_2$, and $2Bi_2O_3 \cdot 3GeO_2$. We measured their ^{209}Bi NQR spectra at 77 and 300 K on a pulsed NQR spectrometer and recorded the resonance line shapes in zero and weak static magnetic fields ($H_{ext} < 500$ Oe) applied perpendicularly to the direction of radio-frequency field (H_{rf}). The line shapes were compared with the results of computer simulations.

The sample of bismuth aluminate $Bi_2Al_4O_9$ (I) consisted of small single crystals, obtained by spontaneous crystallization from a Bi_2O_3 flux, whereas those of $Bi_2Ga_4O_9$ (II) and $Bi_2Ge_3O_9$ (III) were powders. As reported in [5], the crystals I are orthorhombic, space group Pbam (D92h). The Al atoms occupy two sites in the crystal lattice, one in tetrahedral and the other in octahedral environment of oxygen atoms. In the distorted BiO_6 octahedron, the Bi-O distances are 0.213, 0.241, and 0.291 nm. Closely similar X-ray powder diffraction patterns for I and II evidence that the compounds are isostructural.

* Presented at the XIVth International Symposium on Nuclear Quadrupole Interactions, Pisa, Italy, July 20–25, 1997.

Reprint requests to Dr. E. A. Kravchenko; Fax: 7-095-954-1279.

0932-0784 / 98 / 0600-0504 $ 06.00 © – Verlag der Zeitschrift für Naturforschung, D-72027 Tübingen

Bismuth germanate (III) crystallizes in the benitoite-type structure, space group P63/m. The Bi atoms are surrounded by two groups of nearest-neighbor oxygen atoms, three in each group, so that the Bi-O bond lengths are 0.2141 and 0.2743 nm [6].

The ^{209}Bi NQR spectra of I–III were previously unknown. The results of their measurements are given in our short preliminary communication [7] together with the details of preparation.

The samples of $Bi_4Ge_4O_{12}$ were studied as single crystals having different orientation of their crystallographic axes with respect to the H_{rf} direction. In zero magnetic field, the NQR spectra of all the samples were in general agreement with those reported in [8] for 77 K and in [9] for 300 K. We recorded the ^{209}Bi NQR line shape evolution in external magnetic fields ($0 < H_c < 450$ Oe) on the samples IV ($H_{rf} \perp$ (100) plane) and V ($H_{rf} \perp$ (111) plane).

Results and Discussion

The ^{209}Bi NQR spectra of the polycrystalline I, powdered II and III, and single-crystal IV and V samples are given in Table 1. The broadest resonances (up to 500 kHz in width at half-maximum) were observed on $Bi_2Al_4O_9$, although the appropriate sample consisted of small single crystals. The EFG asymmetry parameters reveal an axially symmetric environment of the Bi sites in III and fairly low axial symmetry in I. The ^{209}Bi lines in the spectra of I–III appeared either distinctly split or asymmetric in shape, although the X-ray data [5, 6]evidence that the Bi sites in these compounds are crystallographically equivalent. In the spectra of IV and V, the ^{209}Bi resonances were more narrow than in I–III; the most narrow lines (~50 kHz) were observed in V. Nevertheless, the latter resonances were also either split or asymmetric in zero external magnetic field (Figure 1).

Earlier, the typically Zeeman line splittings were observed in zero external magnetic field in the ^{209}Bi NQR spectra of α-Bi_2O_3, and notably asymmetric line shapes were recorded on Bi_3O_4Br [1] and refs. therein. This suggested the presence of an internal source of the splitting in these compounds, which was concluded to be a local magnetic field (H_{loc}) of the order of 200 G. More recent results of SQUID measurements on α-Bi_2O_3 [3] revealed a very unusual behaviour of its magnetisation, evidencing that the magnetic properties of the compounds are more complicated than they are conventionally thought to be.

Assuming that a similar souce of splittings and line shape asymmetry, namely H_{loc}, is also present in the mixed oxides I–V, we estimated its value and orientation with respect to the q_{zz} direction of the EFG. For this, a computer simulation of the line shape was carried out under the assumption that the spin system of quadrupole nuclei is perturbed by local (H_{loc}) and external (H_e) magnetic fields, so that the combined Hamiltonian is

$$H = H_Q + H_{loc} + H_e, \tag{1}$$

where H_Q is the nuclear electric quadrupole Hamiltonian

$$H_Q = e^2 Q q[3I_{z'}^2 - I(I+1) + \eta/2(I_+^2 + I_-^2)]/[4I(2I-1)], \tag{2}$$

$$H_{loc} = -g_{Bi}\,\mu_B\,\mathbf{H}_{loc}\,\mathbf{I} = -g_{Bi}\,\mu_B\,H_{loc}(\sin\theta_i\cos\phi_i\,I_{x'} + \sin\theta_i\sin\phi_i\,I_{y'} + \cos\theta_i\,I_{z'}). \tag{3}$$

Table 1. ^{209}Bi NQR spectra (MHz) and local magnetic fields (H_{loc}, θ_i, ϕ_i) in mixed oxides. [a] [8]; [b] [9].

Compound	T, K	Transition frequencies averaged over splittings				e^2Qq/h	η, %	H_{loc}, G	θ_i°	ϕ_i°
		1/2 – 3/2	3/2 – 5/2	5/2 – 7/2	7/2 – 9/2					
$Bi_2Al_4O_9$ (I)	77	33.15	50.50	78.03	104.12	626.40	18.6	150 ± 10	0 ± 10	0 ± 5
	300	33.30	49.34	76.40	102.30	615.70	19.7			
$Bi_2Ga_4O_9$ (II)	77	26.12	50.55	76.05	101.43	608.30	5.9	95 ± 10	0 ± 5	–
	300	25.70	49.19	74.20	98.98	593.79	6.8			
$Bi_2Ge_3O_9$ (III)	77	25.74	51.62	77.35	103.17	618.82	0.0	60 ± 10	25 ± 5	–
	300	25.25	50.49	75.73	100.97	605.89	0.0			
$Bi_4Ge_3O_{12}$ (IV), (V)	77	21.15[a]	42.34[a]	63.53[a]	84.68[a]	507.98	0.0			
	300	20.43[b]	40.90[b]	61.28[b]	81.70[b]	490.30	0.0	25 ± 5	45 ± 5	–

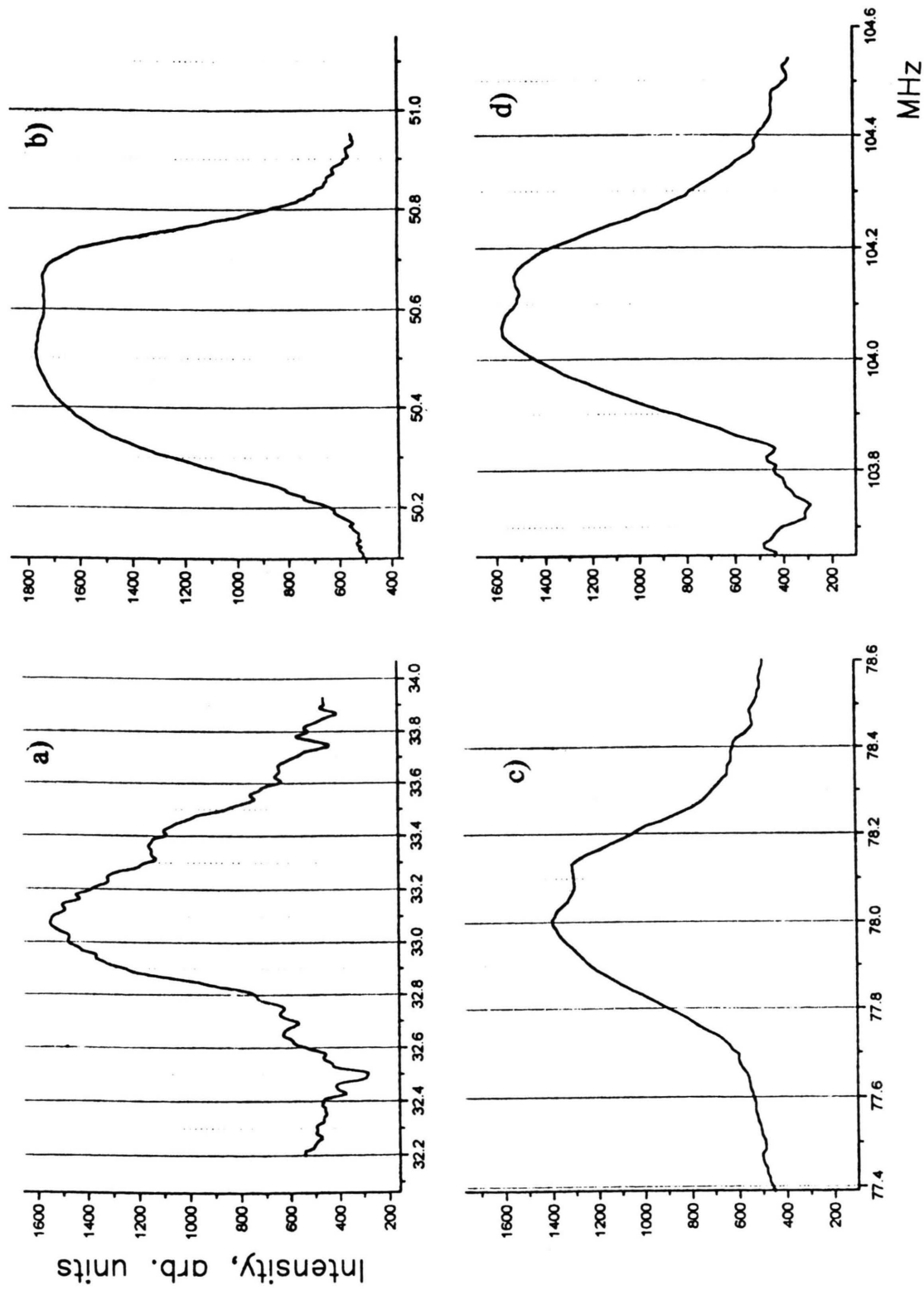
a)
b)
c)
d)
Intensity, arb. units
MHz

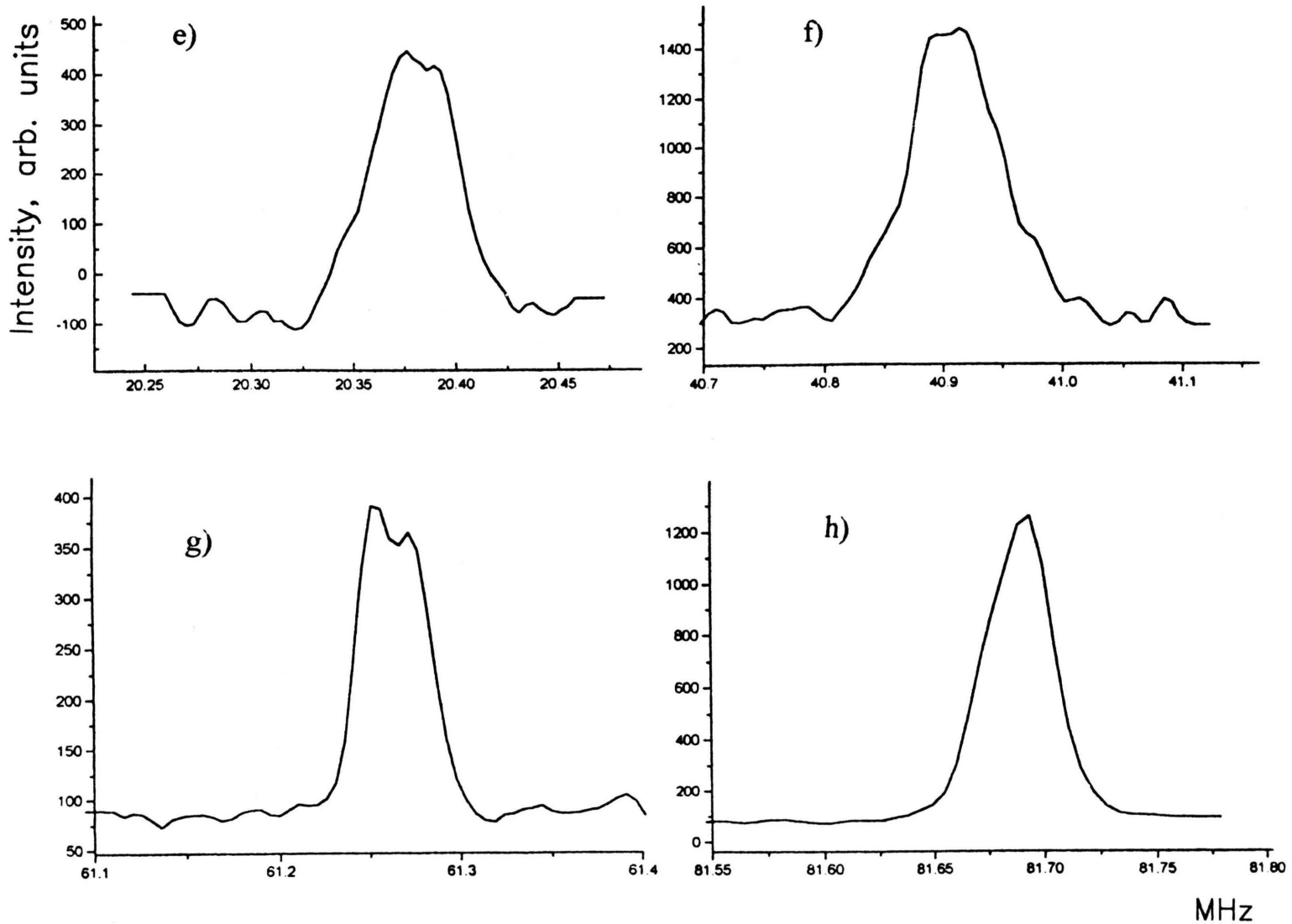

Fig. 1. The zero-field ^{209}Bi line shapes of polycrystalline $Bi_2Al_4O_9$, 77 K (a–d) and single crystal $Bi_4Ge_3O_{12}$, 300 K (e–h): (a) and (e) $\nu_1 = 1/2 - 3/2$; (b) and (f) $\nu_2 = 3/2 - 5/2$; (c) and (g) $\nu_3 = 5/2 - 7/2$; (d) and (h) $\nu_4 = 7/2 - 9/2$.

In (3), θ_i and ϕ_i determine the direction of H_{loc} with respect to the EFG principal axes,

$$H_e = -g_{Bi}\,\mu_B\,\mathbf{H}_e\,\mathbf{I} = -g_{Bi}\,\mu_B\,H_e(\sin\theta\sin\psi I_{x'} + \sin\theta\cos\psi I_{y'} + \cos\theta\,I_{z'}), \quad (4)$$

$g_{Bi} = \mu_{Bi}/(I\,\mu_B)$, $\mu_{Bi} = 4.0797\ \mu_B$, where μ_B is the Bohr magneton.

Here, the laboratory frame (x, y, z) is defined by the applied magnetic field H_e ($\|z$) and the NQR probe coil axis ($H_{rf} \| x$), and the primed coordinates refer to the principal axes of the EFG. The unprimed laboratory frame is connected to the primed EFG principal axis system by rotation about the appropriate axes through the Euler angles ϕ, θ and ψ [10].

In general case ($H_{loc} \neq 0$ and $H_e \neq 0$), the Hamiltonian (1) is the Hermitian operator, whose matrix elements form the complex Hermitian matrix. The real eigen values E_α and complex eigen functions $Y_\alpha(\alpha = 1, 2, \ldots, 10)$ of this matrix were determined by a standard diagonalization procedure. Hence, the nuclear spin energy level E_α is a function of eight parameters: e^2Qq, η, H_{loc}, θ_i, H_e, θ, ψ.

In zero external field, E_α is mainly determined by the first four parameters. If $\eta = 0$, E_α does not depend on ϕ_i; the latter influences the position of four lower energy levels E_α at $\eta \neq 0$ only, the remaining levels being practically insensitive to ϕ_i.

The interaction of H_{rf} with the nuclear spin is given by the square matrix element $\Omega_{\alpha\beta}$, to which the probability for the $E_\alpha \rightarrow E_\beta$ transitions is proportional:

$$\Omega_{\alpha\beta} = |\langle Y_\alpha|\mathbf{H}_{rf}\,\mathbf{I}|\,Y_\beta\rangle|^2 = H_{rf}^2\,\omega_{\alpha\beta}. \quad (5)$$

With the mutual arrangement of the primed and unprimed coordinates taken into account, one obtains

$$\omega_{\alpha\beta} = |\langle Y_\alpha|(\cos\psi\cos\phi - \sin\psi\cos\theta\sin\phi)\,I_{x'} + (-\sin\psi\cos\phi - \cos\psi\cos\theta\sin\phi)\,I_{y'} + \sin\theta\sin\phi\,I_{z'}|Y_\beta\rangle|^2. \quad (6)$$

The appropriate line shape was simulated using the expression

$$F_{\alpha\beta} \propto \nu_{\alpha\beta}^2\,\omega_{\alpha\beta}\int_{\tilde{\nu}_1}^{\tilde{\nu}_2} g(\nu - \nu_{\alpha\beta})\,d\nu, \quad (7)$$

where $\nu_{\alpha\beta} = (E_\beta - E_\alpha)/h$ is transition frequency. In (7), the convolution with a Gaussian

$$g(\nu - \nu_{\alpha\beta}) = \sqrt{4\ln 2}\,/\left(\sqrt{\pi}\sigma\right) \cdot \exp\left[-4\ln 2\,(\nu - \nu_{\alpha\beta})^2/(\sigma^2)\right] \quad (8)$$

was performed, so that σ denotes here a line width at half maximum simulating the effect of EFG broadening.

The entire line shape was simulated by summing all the transitions between E_β and E_α levels, associated with non-zero $\omega_{\alpha\beta}$:

$$S = \Sigma F_{\alpha\beta}. \quad (9)$$

The simulation procedure was as follows: the e^2Qq- and η-values were determined from the NQR transition frequencies, measured in zero external field and averaged over splittings. The values of H_{loc}, θ_i, and ϕ_i were further estimated by a comparison of the simulated patterns with the observed lines, assigned to the transitions $\nu_1 = 1/2 - 3/2, \ldots, \nu_4 = 7/2 - 9/2$. The results of the estimation are given in Table 1.

Upon simulating the line shapes in non-zero magnetic fields, the eigen values E_α and eigen functions Y_α were found from (2)–(4) by varying the angles ϕ, θ, and ψ at the given values of e^2Qq, η, H_{loc}, θ_i, ϕ_i, and H_e. This enabled to calculate $\omega_{\alpha\beta}$ (6), $F_{\alpha\beta}$ (7), and the entire line shape S (9), expected in different applied magnetic fields.

For the powder patterns, ϕ and ψ were varied with steps of 2° from 0 to 360°, and θ from 0 to 180°, followed by the summation of all the spectra. Hence, the resulting simulated line shape was an average of this sum. Because the width σ of the Gaussian (8) is finite, a further decrease of the step did not influcence the line shape.

In Fig. 2, the simulated line shapes ν_1 and ν_2 in the powdered samples II and III, respectively, are compared to the observed evolution of the same lines in external magnetic fields.

The samples IV and V were, as mentioned above, single crystals of $Bi_4Ge_3O_{12}$ having different orientations of the crystallographic axes with respect to the x-axis of the laboratory frame ($x \| H_{rf}$). In IV, the latter axis was perpendicular to a (100) crystallographic plane, and in V, to a (111) plane.

The computer simulation procedure for the single crystal patterns was similar to the above-described, with the difference that no averaging over the angle parameters was performed. In zero H_e, the line shapes were insensitive to the ϕ, θ, and ψ, and the varying of the latter angles influenced the line intensities only. In non-zero H_e, the energies E_α depended on θ, if $\eta = 0$. The values of σ in (8) were taken in consistence with the observed line widths, i.e., between 0.025 and 0.2 MHz. In (7), the interval ($\tilde{\nu}_2 - \tilde{\nu}_1$) between the integration limits was divided into 200 boxes. A further increase in number of boxes did not improve the results of simulation.

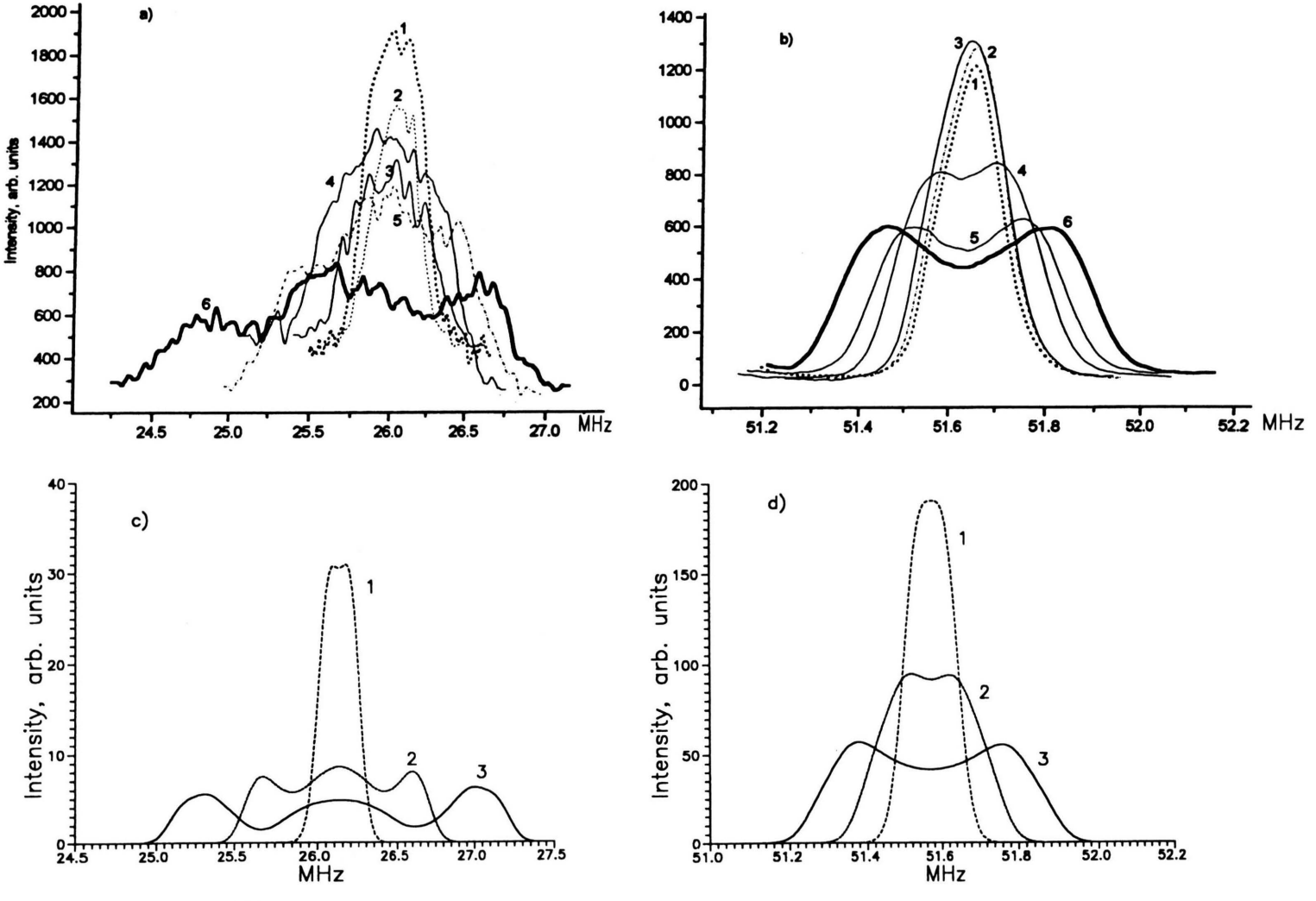

Fig. 2. The evolution of the ^{209}Bi line shapes in external magnetic fields observed on $Bi_2Ga_4O_9$, ν_1 (a), and $Bi_2Ge_3O_9$, ν_2 (b) as compared to the results of simulation (c and d, respectively). The numbering of curves denotes the magnetic fields H_e (Oe): (a) 1: 0, 2: 30, 3: 120, 4: 180, 5: 270, 6: 390; (b) 1: 0, 2: 60, 3: 90, 4: 210, 5: 300, 6: 390; (c and d) 1: 0, 2: 200, 3: 400.

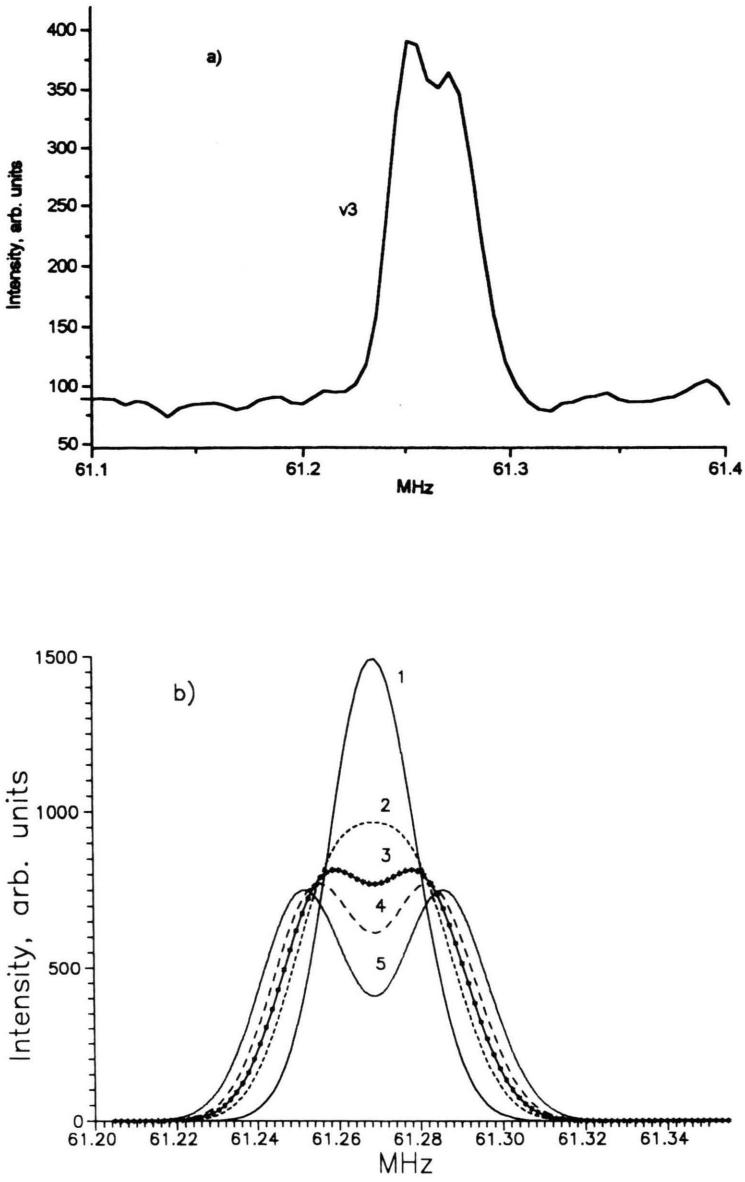

Fig. 3. Recording of the zero-field ^{209}Bi resonance $\nu_3 = 5/2 - 7/2$ in $Bi_4Ge_3O_{12}$ (V) (a) and the simulated pattern (b) that demonstrates the sensitivity of the pattern to H_{loc} and θ_i: 1: $H_{loc} = 0$; 2: $H_{loc} = 25$ G, $\theta_i = 55°$; 3: $H_{loc} = 25$ G, $\theta_i = 45°$; 4: $H_{loc} = 25$ G, $\theta_i = 35°$; 5: $H_{loc} = 35$ G, $\theta_i = 45°$.

Figure 3 illustrates the sensitivity of the simulated pattern (the transition $\nu_3 = 5/2 - 7/2$ in the spectrum of V) to H_{loc} and θ_i. One can see that the curve 3 (Fig. 3b) is in the best agreement with the results of the zero-field experiment.

In non-zero magnetic field, the results of the simulation of the lower-transition resonance $\nu_1 = 1/2 - 3/2$ in $Bi_4Ge_3O_{12}$ give a quartet of lines, symmetrical about the zero-field NQR frequency, whereas doublets are expected for the remaining transitions (Fig. 4a, b). The experiment, however, gave a more complicated picture. As seen in Fig. 5, the multiplicity of the ν_1 line in the ^{209}Bi NQR spectra of both $Bi_4Ge_3O_{12}$ single-crystal samples exceeded 6 in the external fields above 300 Oe. The higher-transition lines in their spectra also showed the multiplicity, which was twice or three times as high as that in the simulated patterns. It should be noted, however, that the frequency intervals between the edge lines of the

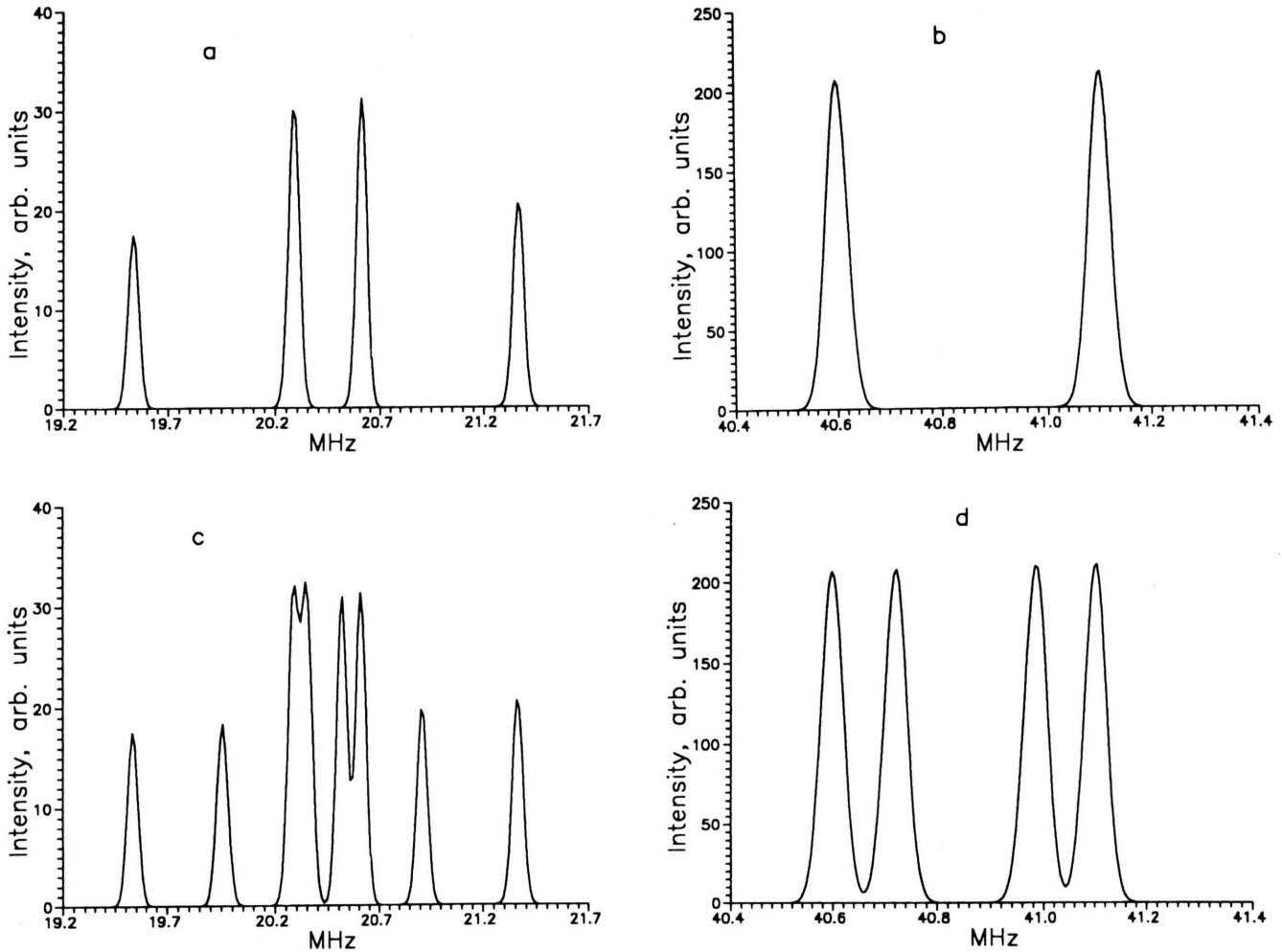

Fig. 4. The simulated single-crystal patterns ν_1 (a) and ν_2 (b) in the spectrum of $Bi_4Ge_3O_{12}$ in H_e = 450 Oe and superimposed simulated patterns of the same transitions (c and d, respectively) in H_e = 450 and 200 Oe.

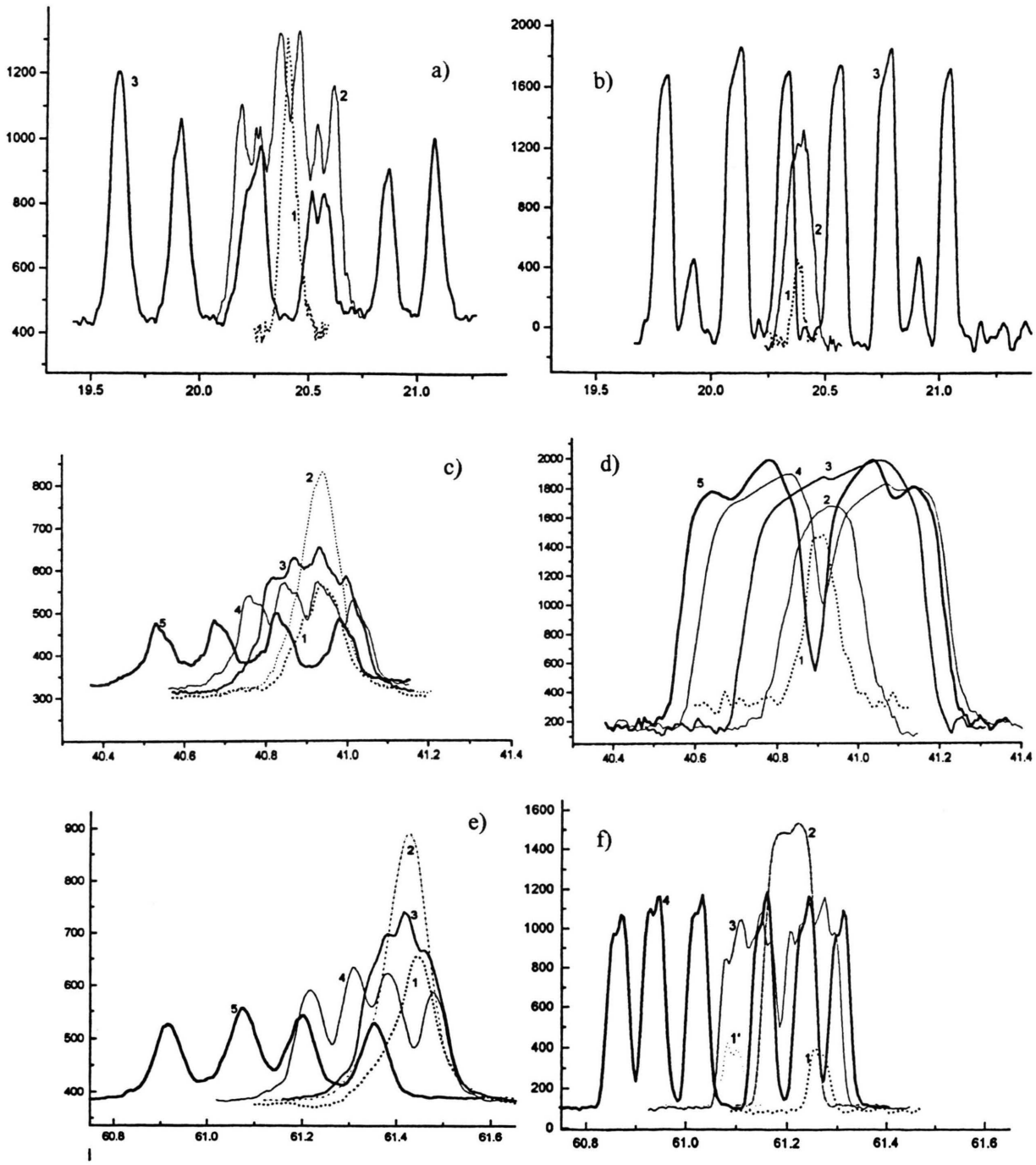

Fig. 5. Recording of the ^{209}Bi $\nu_1 - \nu_3$ line shape evolution (the upper-middle-bottom rows, respectively) in static magnetic fields on the $Bi_4Ge_3O_{12}$ samples IV (left columns) and V (right column). The numbering of curves denotes the magnetic fields H_e (Oe): (a) 1: 0, 2: 110, 3: 450; (b) 1: 0, 2: 30, 3: 300; (c) 1: 0, 2: 50, 3: 110, 4: 270, 5: 450; (d) 1: 0, 2: 10, 3: 240, 4: 360, 5: 420; (e) 1: 0, 2: 50, 3: 110, 4: 270, 5: 450; (f) 1 and 1': 0, 2: 60, 3: 180, 4: 420. (1 denotes the curve before H_e was switched on, and 1', after H_e was switched off).

simulated patterns in non-zero fields were in good agreement with the appropriate intervals, observed in the experiments in the same fields.

This might evidence that both crystals contain domains, characterized by net magnetic fields ($H_{loc} + H_e$) of different magnitudes. In such a case, the observed NQR spectrum of the crystal can be modeled by a superposition of the spectra of the constituting domains, one of which being characterized by the applied field H_e and the others (their number is associated with the multiplicity of the spectrum), the relatively reduced fields. An attempt to simulate the spectral patterns ν_1 and ν_2, observed on the sample IV in $H_e = 450$ Oe (Fig. 5a, c), as a superposition of two patterns, calculated at $H_e = 450$ Oe and $H_e = 200$ Oe (the remaining parameters being $e^2Qq/h = 490.25$ MHz, $\eta = 0$, $H_{loc} = 25$ Oe, $\theta_i = 45°$, $\phi_i = 0°$, $\phi = 45°$, $\theta = 40°$, $\psi = 45°$), gave the results plotted in Fig. 4c, d. Similarly, the spectra observed on the sample V in $H_e > 300$ Oe, which seem to comprise the threefold number of components a s compared to that expected (Fig. 5b, d, f), could be simulated by a superposition of three sets of lines calculated, using the above parameters, for $H_e = 140$, 280, and 420 Oe, which corresponds to the presence of three types of domains. This suggestion is, however, speculative and needs more data for its verification.

It is interesting that the ^{209}Bi resonance intensities in the spectra of all the samples exhibited a very unusual behavior in static magnetic fields, most prominent in the spectrum of V. On application of the magnetic field, the intensity of the resonances increased strongly, so that the net signal in the external field exceeded the zero-field signal by orders of magnitude (Figure 5). The comparison of the data on the samples IV and V shows, that the mutual orientation of q_{zz}, H_{loc}, H_e, and H_{rf} is a factor of primary importance for the observation of this effect. Unfortunately, no attempts to simulate the intensity increase under the influence of H_e gave conclusive results. The mechanism of this effect, as well as the origin of H_{loc} in the Main Group element oxides, remains still unclear. The present data support, however, our earlier suggestion [1] that this phenomenon is not unique and may be found in other compounds, if the experiments are performed in relatively weak (below 1 kOe) magnetic fields.

Conclusions

The internal sources of splitting in the zero-field ^{209}Bi NQR spectra seem to exist, in addition to α-Bi_2O_3 and Bi_3O_4Br, in $Bi_2Al_4O_9$, $Bi_2Ga_4O_9$, $Bi_2Ge_3O_9$, and $Bi_4Ge_3O_{12}$. These are suggested to be the local magnetic fields, whose values and orientations with respect to the EFG principal axes were estimated using computer simulation. The patterns simulating the NQR line shape evolution in weak static magnetic fields are in satisfactory agreement with the experiments.

Higher than expected multiplicity of the lines in applied magnetic fields was observed on $Bi_4Ge_3O_{12}$ single crystals having different orientation of the crystallographic axes with respect to H_{rf}. This observation is, to the author's knowledge, the first of its kind. The most probable explanation for this finding is the existence of domains, characterized by different internal magnetic fields.

A notable increase in intensity of the resonances was observed upon applying magnetic fields. The largest increase was observed on the $Bi_4Ge_3O_{12}$ single crystal whose crystallographic plane (111) was perpendicular to H_{rf}. The mutual orientation of the fields influencing the nuclear spin system seems to make an important contribution to this effect.

Acknowledgement

We are grateful to the Russian Foundation for Basic Research for the support, project N° 96-03-34238. Two of us, E. A. K. and S. H. F. are grateful to A. A. Gippius for technical assistance.

[1] E. A. Kravchenko and V. G. Orlov, Z. Naturforsch. **49a**, 418 (1994); N. E.Ainbinder, G. A. Volgina, E. A. Kravchenko, A. N. Osipenko, A.A. Gippius, Suan Hai Fam, and A. A. Bush, Z. Naturforsch **49a**, 425 (1994).
[2] V. N. Duginov, V. G. Grebinnik, V. G., T. N. Mamedov, et al., Hyperfine Interactions **85**, 197 (1994).
[3] A. I. Kharkovskii, V. I. Nizhankovskii, E. A. Kravchenko, and V. G. Orlov, Z. Naturforsch. **51a**, 665 (1996).
[4] V. G. Orlov, A. A. Bush, S. A. Ivanov, and V. V. Zhurov, J. Low Temperature Physics **105**, (5/6), 1541 (1996).
[5] N. Niizeki and M. Wachi, Z. Kristallogr. **127**, 173 (1968).
[6] B. C. Grabmaier, S.Haussühl, and P. Klufers, Z. Kristallogr. **149**, 261 (1979).
[7] E. A. Kravchenko, Fam Suan Hai, and Yu. F. Kargin, Neorg, Mater. **33**, 1001 (1997).
[8] Yu. A. Buslaev, E. A. Kravchenko, and L.Kolditz, Coord. Chem. Rev. **82**, 1 (1987).
[9] K. V. Gopalakrishnan, L. G. Gupta, and R. Vijayaraghavan, Pramana **6**, 343 (1976).
[10] E. D. von Meerwall, R. B. Creel, C. F. Griffin, and S. L. Segel, J. Chem. Phys **59**, 5350 (1973).